


## A new probabilistic hybrid segmentation technique

Suat Karakaya<sup>1,a\*</sup> 

<sup>1</sup>Kocaeli University, Engineering Faculty, Mechatronics Engineering Department, Kocaeli, Türkiye

\*Corresponding author: suat.karakaya@kocaeli.edu.tr

(Received: June 9, 2023 / Accepted: July 14, 2023)

### Abstract

The aim of this study is to propose a probabilistic contour determination method on indoor map scan data. Traditional probabilistic contour detection algorithms operate as a kind of decision-making tool by processing the segment between two randomly selected samples in a full dataset. Pure geometric approaches, on the other hand, focus on identical features (corners, landmarks etc.) with a series of labeling operations based on Euclidean distance. Both approaches are commonly used in the literature to recognize a predefined geometric pattern. At the core of this study, a novel segmentation and labelling strategy is performed in a manner that geometrical and probabilistic principles are applied sequentially. In the first stage, the total data segmented with the line splitting strategy is transformed into subsets from which random samples will be selected in the following steps. Samples selected from the new (constrained) subsets provide higher accuracy segmentation. The data set processed in the study are indoor distance measurements obtained from the 2D Light Detection and Ranging (LIDAR) sensor. The detected line segments are one of the most basic features used for indoor positioning and the results of the study can be adapted to indoor positioning systems.

**Keywords:** pattern recognition; signal processing; robotics

### Introduction

Pattern recognition methods are widely used in robot control and computer vision fields. The data forming the initial pattern is usually obtained from an external sensor. In the current literature, mobile robot systems operating in indoor conditions are majorly equipped with 2D laser sensors (LIDAR) to solve localization and collision-free navigation problems. The operations such as obstacle detection, feature extraction, mapping, localization and moving object detection can be carried out by processing the LIDAR measurements. Variety of algorithms in the literature offer solutions to these problems based on the measurement model of these sensors. LIDAR measurements can be processed based on point feature extraction [1-4] or linear feature extraction [5-6]. However, in laser-based systems, negative effects (scattered data, bad reflections, refractions, etc.) lead to noisy samples. In this case, feature extraction with purely geometric approaches based on ideal situations becomes impractical. More robust techniques are required to solve such challenging problems. With this perspective, Hough transform is implemented as a robust technique [7]. With this technique, infinite line segments can be extracted from the 2-dimensional data set [8]. To find the exact solution, it is necessary to limit the infinite segments, for this purpose, several novel methods have been put forward [9-11]. Similarly, a method has been proposed for moving sensor models using a non-stochastic approach, and segmentation can be performed in dynamic conditions [12]. Original studies have also been conducted in robotic positioning systems investigating measurement clouds corresponding to artifacts [13]. As a probabilistic method, Random Sample Consensus (RANSAC) has been used in the literature for contour detection, lane tracking and linear feature extraction [14-16]. In RANSAC-based methods, a random parameter set is created and the parameter that best expresses the data is selected from this set. Thus, the dataset is modeled. RANSAC can be defined as a resampling method that provides possible solutions using the minimum number of data points needed to estimate desired model. RANSAC does not progress an outlier filtering preprocess but due to its characteristic of extracting lines randomly and the respective group extraction an overlapping check is required. On the other hand, the advantage of the RANSAC algorithm is that it is fast. The maximum number of iterations does not depend on the size of measurement, but only on probabilities that must be defined in advance. The number of points is important only for finding points that fit an estimated line. Split&Merge method, which is one of the geometric approaches, is also an effective

method applied in the line detection process [17-20]. The basic principle of this approach is based on the detection of breakpoints of linear patterns hidden on the data set consisting of measurement points. However, the "Splitting" part, which is the first stage of this method, is not sufficient for a correct segmentation. Management of outlier data cannot be satisfied by implementing only "Splitting" operation. Split & Merge utilizes whole data of the given measurement so it's necessary to implement an outlier filtering. The progressing the outlier data filtering is carried out by implementing the "Merge" process which is the second stage of the overall algorithm. The segment overlapping does not occur as it processes every single point once and clusters the points systematically. Douglas-Peucker Algorithm is a line fitting and point reduction algorithm [21]. The algorithm takes as input a set of points that define a curve and a tolerance value. It returns the subset of the original dataset, which is formed because of deleting the points that are closer to each other than the tolerance value, considering the order of the points as output [22]. Even though the method has certain advantages; It has weaknesses such as omission of some feature points, self-intersection when graphs are complex or when the threshold is large, the common boundary of two adjacent curves is inconsistent [23].

To simplify the diversity in the literature, segmentation processes can be divided into two basic categories: Point-distance-based and Kalman filter-based segmentation methods. In this study, a point-distance-based scheme was studied, and segmentation was performed with geometric relations on LIDAR data.

In this study, the first part of the Split&Merge algorithm (Splitting) and the RANSAC algorithm were implemented sequentially, combining the strengths of both methods. A hybrid version of these two geometric and probabilistic methods is presented. Detailed information about both approaches is explained under the title "Theoretical Background". The results of the proposed technique are presented in the Results section.

## Materials and Methods

### LIDAR measurement model

LIDAR data is a distance measurement vector. The elements of the vector are the distances in millimeters between the sensor focal center and the surface hit by the laser source. The number of distance measurements depends on the angular resolution of the sensor. For example, if a sensor with a  $180^\circ$  angle of view takes measurements with a resolution of  $1^\circ$ , a sequentially 181-elements vector will be obtained for each obstacle in the angular position of  $0^\circ$  and  $180^\circ$ .

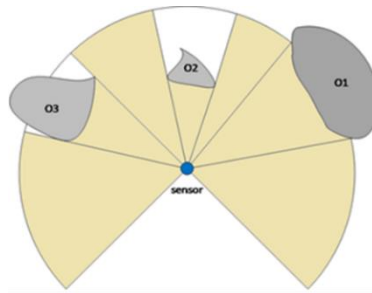


**Figure 1.** LIDAR measurement model

In Figure 1, obstacles positioned at random positions within the LIDAR scanning range in two-dimensional space and the LIDAR scanning section are given schematically. Areas highlighted in dark tone indicate areas where LIDAR beams can hit and take measurements. The closed regions labeled with the symbol "O" represent obstacles.

The LIDAR measurement model is given in (1), where  $p_L$  illustrates the position of the sensor in global space;  $\alpha$  and  $r_L$  demonstrate the angle position of the measurements and the maximum measurement range of the sensor respectively.

$$m(p_L, \alpha) = \min_{\gamma \in [0, r_L]} \left( p_L, p_L + \gamma \begin{bmatrix} \cos(\alpha) \\ \sin(\alpha) \end{bmatrix} \right), \quad \left( p_L, p_L + \gamma \begin{bmatrix} \cos(\alpha) \\ \sin(\alpha) \end{bmatrix} \right) \in \cup_O \quad (1)$$

For the measurement points where there is no obstacle in the maximum measurement range in the LIDAR model given in Figure 1, the value of the  $r_L$  parameter is assigned to the relevant point. This saturation process is given in (2).

$$m(p_L, \alpha) = \begin{cases} m(p_L, \alpha), & m(p_L, \alpha) < r_L \\ r_L, & m(p_L, \alpha) \geq r_L \end{cases} \quad (2)$$

The diagram given in Figure 2 shows how the data set to be segmented will be obtained from the LIDAR model. The red points indicated by  $m$  represent the limits where the lidar maximum measuring range is exceeded. The consecutive measurement points within the maximum range are used as the feature search space. The notation used in the segmentation scheme given in Figure 2 is explained in Table 2.

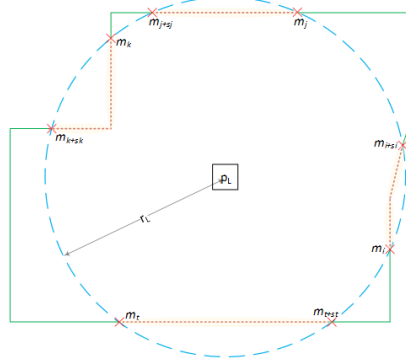


Figure 2. Processed measurement data set

Table 1. Definition of the measurement data scheme

Symbol	Definition
-----	Sections in measurement range
<span style="border: 1px solid black; padding: 2px;"><math>p_L</math></span>	LIDAR position
—————	Sections out of measurement range
-----	Measurement limits

Assuming the maximum range is represented by  $r_L$ , the approach applied for the elimination of partial data sets constituting the feature search space is given in (3) and (4).

$$\beta \in [0 S_i]^{Z^+}, m(i + \beta) \leq r_L \quad (3)$$

$$(\exists m_{i+\beta} \geq r_L | \beta \in [0 S_i]^{Z^+}) = \emptyset \quad (4)$$

The measurement points at a distance less than  $r_L$ , which provide continuity between the maximum range crossing points, are modeled in (3) and (4). The dataset to be processed in further steps is presented as  $(m_i \sim m_{i+\beta})$  groups.

### Polyline Splitting

This method recursively scans the vertices in the total dataset. The endpoints of each segment are the corner positions detected in the dataset. These lines may not be the final segments, because a precise linear geometry cannot be found without the "merge" operation. In other words, the Splitting stage is a pre-process for the "Merge" stage. The set of points between the detected vertices is considered a candidate line segment. The measurement at the furthest Euclidean distance from the fundamental line drawn between the start and end of the data set is considered a new vertex. This vertex creates two new lines, and this process continues to be applied recursively to the new line segments. If any measurement point between the endpoints is not further than a certain threshold value, the algorithm is stopped, and the "Splitting" phase is completed. An example diagram showing the processing steps of the algorithm is given in Figure 3.

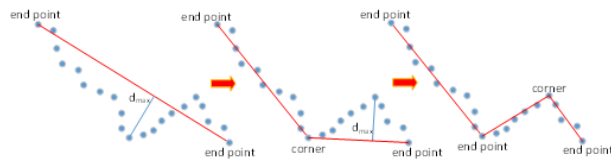


Figure 3. Line splitting scheme

The flowchart of the line splitting algorithm is given in Figure 4.

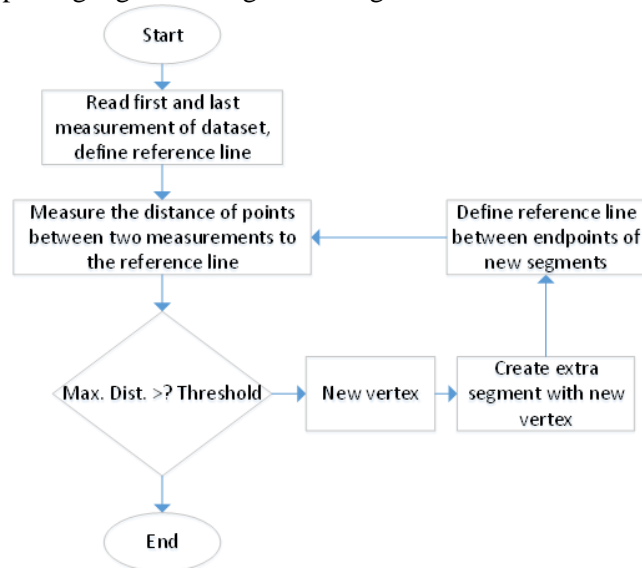


Figure 4. Line splitting flowchart

**RANSAC**

RANSAC randomly selects measurements to determine a line and detects measurements within a predefined threshold distance from the candidate line. It is evaluated whether the selected points have the potential to form a possible line segment. Since the threshold value determined to make this decision is highly correlated with the measurement model of the system, it is not possible to determine a generalized value. Depending on the model of the sensor used and the obstacle profile of the environment, this threshold value can be determined based on the system being studied.

RANSAC operation can be summarized in the following steps:

- Measurement data set:  $\{K\}$  and Potential line segment subset:  $\{K_c\}$ ,
- Decision threshold value for subset  $\epsilon \rightarrow N = |K_c|$  must be greater than a limit value ( $N_{min}$ ). This value can be defined as the minimum number of consecutive measurement data that can form a valid line segment in real-world space.
- If the  $N$  value is large enough, the subset  $K_c$  is subtracted from the set  $K$ . A new reduced dataset remains  $\{K_i = K - K_c\}$ . If the value of  $N$  is less than  $N_{min}$ , the steps are repeated using the set  $K$ .
- In case of  $|K_i| < N_{min}$  or if the total number of iterations exceeds a predetermined number, the algorithm is terminated.

An example of a successful iteration providing these steps is given in Figure 5.

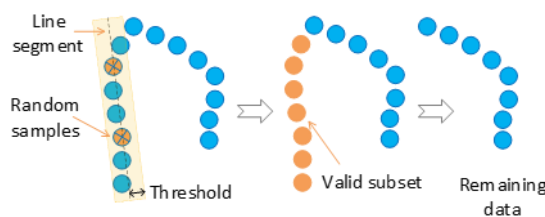


Figure 5. A successful iteration

A probabilistic approach can be put forward to estimate the maximum number of iterations ( $k_{max}$ ) to determine the segments compatible with the line model.

- If the ratio of the data that does not fit the model (No : outlier number) to the total number of measurements (No / K) is considered as the outlier measurement ratio (e), the probability of a measurement data finding a segment suitable for the model can be accepted as  $1 - e$ .
- Since the minimum number of measurements required to define the correct model is 2, this probability is evaluated as  $(1 - e)^2$ .
- In this case, the probability of failure for a measurement step is  $1 - (1 - e)^2$ .
- If the probability of success of the algorithm in the total running time is defined as  $s$ , the probability of success after  $m$  iterations will be  $(1 - s) = (1 - (1 - e)^2)^m$ .

To calculate the number of  $m$  iterations:

- The equation  $\log(1 - s) = m \cdot \log(1 - (1 - e)^2)$  will be converted into  $m = \log(1 - s) / \log(1 - (1 - e)^2)$ .

According to this result, the increase in the measurement rate (e) and the success rate (s) against the correct segment model increase the number of iterations required (m).

**Splitting with RANSAC Extension**

Although splitting can make an effective classification, it may cause underestimation in some special cases. The scenario in Figure 6 can be given as an example of these situations caused by outlier data.

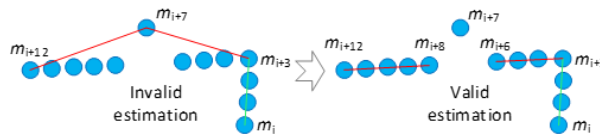


Figure 6. Line splitting & RANSAC

The algorithm given in Figure 4 can accept an outlier measurement data as the start and/or end point of a line segment. These situations may result in poorly segmented maps. An example of this situation is given in Figure 6 and the contribution of the proposed approach is presented on this scenario. The measurement at the maximum distance from the initial segment  $|m_i m_{i+12}|$  becomes  $m_{i+7}$ , and in the next step the new vertex is calculated as  $m_{i+3}$ . Thus,  $|m_i m_{i+3}|$ ,  $|m_{i+3} m_{i+7}|$  and  $|m_{i+7} m_{i+12}|$  are considered as final line segments. However, as seen in Figure 6,  $|m_{i+3} m_{i+7}|$  and  $|m_{i+7} m_{i+12}|$  segments are not optimal in terms of data density. Therefore, RANSAC was applied on the data subsets between the boundaries of each segment. As a result, point  $m_{i+7}$  is implicitly filtered and the final optimal line segments  $|m_i m_{i+3}|$ ,  $|m_{i+3} m_{i+6}|$  and  $|m_{i+8} m_{i+12}|$  has been determined.

**Results and Discussion**

The results of the proposed method in the study will be presented in this section. The data used for experimental studies were obtained using LMS-100 series LIDAR. The maximum scanning angle of the sensor used is  $270^\circ$ , the minimum angular resolution is  $0.5^\circ$  and the maximum range is 20 meters. First, line splitting was applied on the data taken from the indoor map, and then the decomposed data set was post-processed with RANSAC. The same interior data was processed with pure-polyline splitting, and the resulting segments are presented. Both approaches were compared in terms of mean square error of segments.

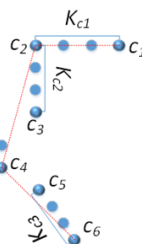
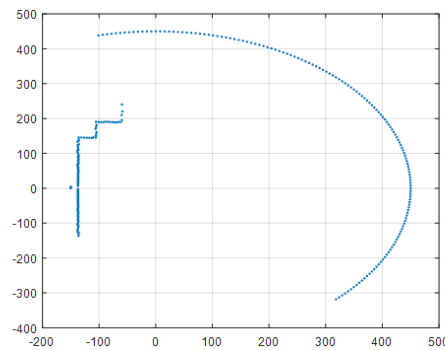
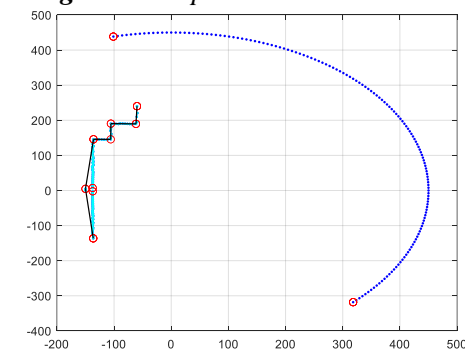


Figure 7. RANSAC searching sets ( $K_{c_1, 2, 3, \dots, n}$ )

The logical procedure applied for the segmentation process is expressed in (5). Since the LIDAR scan angle is  $270^\circ$ , the measurement data is indexed in the range of 1 to 271. Each vertex of the extracted lines becomes an element of the total data set ( $K$ ). In cases where there is at least 1 measurement data located between consecutive vertices, this subset of measurements between the vertices is assumed as a searching set ( $K_c$ ) for RANSAC. The main purpose of this approach is to make groups with denser data become sub-solution sets to find line segments and to increase the probability of best fitting. As the probability of finding dominant lines is high, outlier vertices can be filtered at a higher rate. The outputs of the polyline splitting method on the sample measurement data given in Figure 8 are presented in Figure 9. The outputs of the extended RANSAC implementation are shown in Figure 10. The proximity of the line segments formed in both scenarios to the discrete measurement points at the boundaries of the relevant segment was observed according to the Euclidean distance metric.



**Figure 8.** Experimental data - #1



**Figure 9.** Experimental data - #1 (polyline splitting)

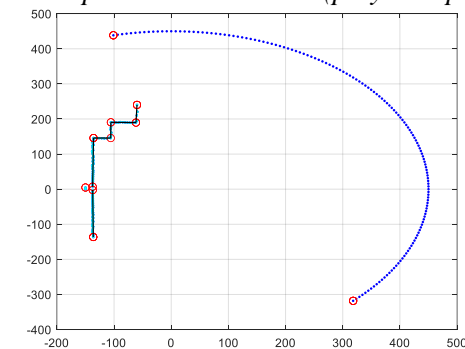


**Figure 10.** Experimental data - #1 (extended RANSAC)

The outputs of the polyline splitting method on the sample measurements given in Figures 11, 14 and 17 are presented in Figures 12, 15 and 18, respectively. The outputs of the extended RANSAC application are shown in Figures 13, 16 and 19, respectively.

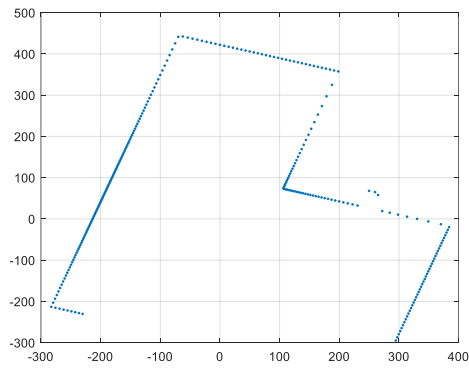


Figure 11. Experimental data - #2

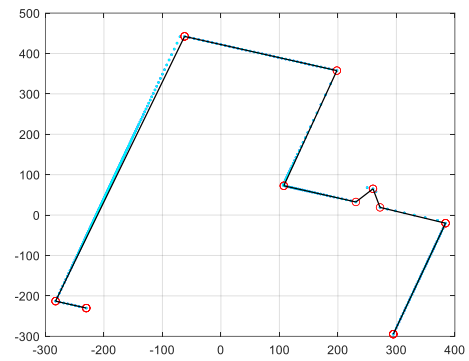


Figure 12. Experimental data - #2 (polyline splitting)

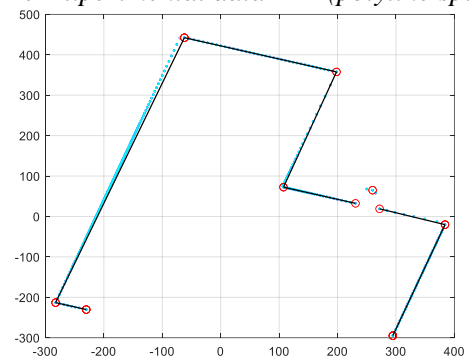


Figure 13. Experimental data - #2 (extended RANSAC)

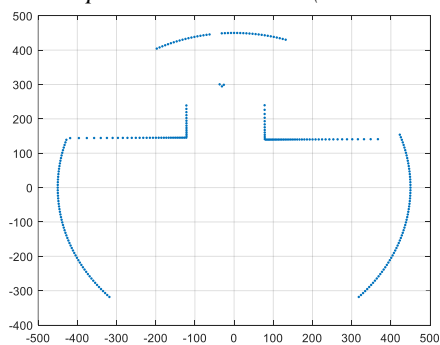


Figure 14. Experimental data - #3

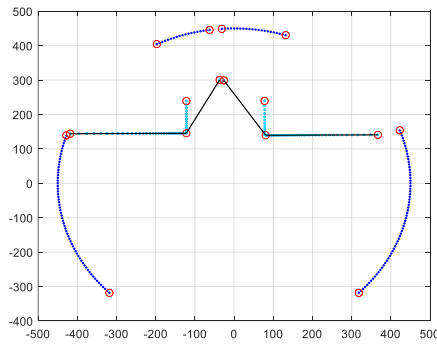


Figure 15. Experimental data - #3 (polyline splitting)

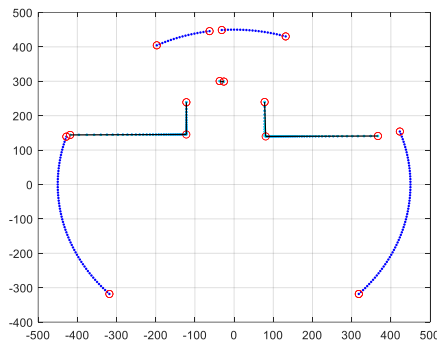


Figure 16. Experimental data - #3 (extended RANSAC)

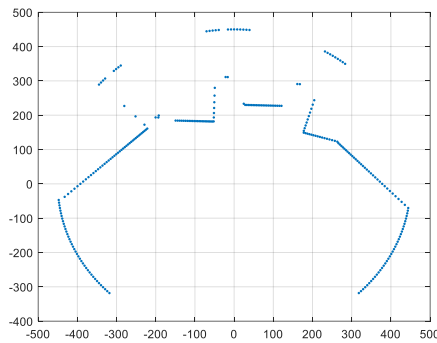


Figure 17. Experimental data - #4

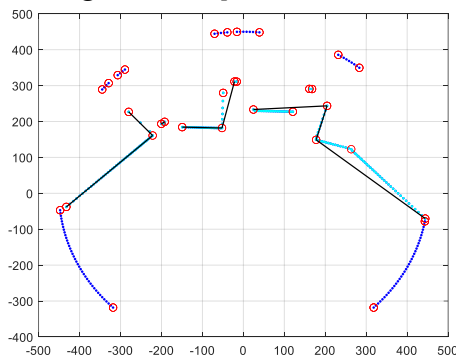
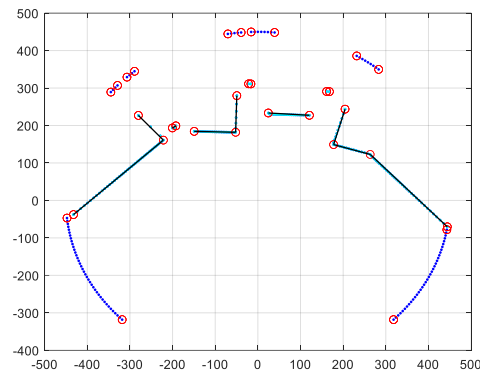


Figure 18. Experimental data - #4 (polyline splitting)





**Figure 19.** Experimental data - #4 (extended RANSAC)

The results prove that the RANSAC extension makes a significant contribution to the current method in terms of segmentation accuracy. The effect of extension is presented in Table 2 as the mean squared error between the measurement data and the line model for the given scenarios.

**Table 2.** Comparative presentation of the methods ( $d_{max}$  given in Fig 3)

	Extended RANSAC	Polyline splitting
$e$ - (Euclidian) [cm] (Experimental data-1)	0.4956	4.7544 ( $d_{max} = 15$ )
$e$ - (Euclidian) [cm] (Experimental data-2)	1.5517	1.5632 ( $d_{max} = 10$ )
$e$ - (Euclidian) [cm] (Experimental data-3)	0.2425	45.5215 ( $d_{max} = 200$ )
$e$ - (Euclidian) [cm] (Experimental data-4)	0.4795	14.5248 ( $d_{max} = 140$ )

The results show that the error levels for different scenarios can be both significant and insignificant. This is because the ratio of the number of data included in the error analysis to the total number of data is relatively low in some scenarios. For example, in the scenario given in Measurement-2, the ratio of outlier data to total data is around 2.15%, which is the reason for the insignificant improvement. Another reason is that the polyline splitting method considers the farthest bounding measurement as the corner point. The ratio of outlier data to total data increases in Measurements 1, 3 and 4, therefore, more significant improvement is observed in RANSAC.

## Conclusions

Geometric methods and probabilistic methods both have distinct advantages. These expected advantages can be easily observed by adapting both approaches to measured data independently. However, a higher accuracy can be obtained when the problem is solved with a hybrid logic. Euclidean distance of the outliers to reference line segments are assumed to be the accuracy metric. it is observed that these distances are shorter than the standard geometric and probabilistic approaches.

## Acknowledgements

This work was supported by Machine Vision Laboratory of Mechatronics Engineering Department.

## References

- [1] V. Nguyen, A. Martinelli, N. Tomatis, R. Siegwart, A comparison of line extraction algorithms using 2D laser rangefinder for indoor mobile robotics, *IEEE/RSJ International Conference on Intelligent Robots and Systems*. (2005) 1929-1934.
- [2] A. Siadat, A. Kaske, S. Klausmann, M. Dufaut, R. Husson, An optimized segmentation method for a 2D laser-scanner applied to mobile robot navigation, *IFAC Symp. on Intelligent Components and Instruments for Control Applications*. (1997) 153–158.
- [3] J. Vandorpe, H. van Brussel, H. Xu, Exact dynamic map building for a mobile robot using geometrical primitives produced by a 2D range finder, *IEEE International Conference on Robotics and Automation*. (1996) 901–908.
- [4] L. Zhang, B. K. Ghosh, Line segment-based map building and localization using 2D laser range finder, *IEEE International Conference on Robotics and Automation*. (2000) 2538–2543.
- [5] L. Tamas, G. Lazea, M. Popa, I. Szoke, Laser based localization techniques for indoor mobile robots, *IEEE International Conference on Advanced Technologies for Enhanced Quality of Life*. (2009), 169-170.
- [6] P. Skrzypczynski, Building geometrical map of environment using IR range finder data, *Intelligent Autonomous Systems*. (1995), 408–412.
- [7] M. Fokkinga, The Hough transform, *Journal of Functional Programming*, Cambridge University Press. (2011), 129-133.
- [8] F. Xiao, L. Jin, W. Haopeng, A study of image retrieval based on Hough transform, *IEEE Computer Science and Information Technology (ICCSIT)*. (2010), 94-98.
- [9] K. Khoshelham, Extending generalized Hough transform to detect 3D objects in laser range data, *ISPRS Workshop on Laser Scanning*. (2007), 206-210.
- [10] J. Forsberg, U. Larsson, A. Wernersson, Mobile robot navigation using the range-weighted Hough transform, *IEEE Robotics and Automation Magazine*. (1995), 18–26.
- [11] W. Zhang, W. Guo, S. Zhao, An improved method for spot position detection of a laser tracking and positioning system based on a four-quadrant detector, *Sensors*. (2019), 1-19.
- [12] N. E. Pears, Feature extraction and tracking for scanning range sensors, *Robotics and Autonomous System*. (2000), 43–58.
- [13] Y. D. Kwon, J. S. Lee, A stochastic environment map building method for mobile robot using 2-D laser range finder, *Autonomous Robots*. (1999), 187–200.
- [14] Y. Hu, Y. Kim, K. Lee, S. Ko, Lane detection based on guided RANSAC, *Proc. of the International Conference on Computer Vision Theory and Applications*, (2010), 457-460.
- [15] J. Liu, F. Bu, Improved RANSAC features image-matching method based on SURF, *J. Eng.* (2019), 9118-9122.
- [16] H. Sheng, Y. Gao, B. Zhu, K. Wang, X. Liu, Feature extraction of SAR scattering centers using M-RANSAC and STFRFT-based algorithm, *EURASIP Journal on Advances in Signal Processing*. (2016), 1-16.
- [17] Y. Xiao, J. Zou, H. Yan, An adaptive split-and-merge method for binary image contour data compression, *Pattern Recognition Letters*. (2001), 299-307.

- [18] D. Karatzas, A. Antonacopoulos, Text extraction from Web images based on a split-and-merge segmentation method using colour perception, *Proceedings of the 17th International Conference on Pattern Recognition*. (2004), 634-637.
- [19] Z. Man, W. Ye, P. Lou, H. Xiao, Feature extraction based on split-merge in range image of LIDAR, *Chinese Journal of Mechanical Engineering*. (2011), 2303-2306.
- [20] A. Y. S. Chia, S. Rahardja, D. Rajan, M. K. Leung, A Split and merge based ellipse detector with self-correcting capability, in *IEEE Transactions on Image Processing*. (2011), 1991-2006.
- [21] U. Ramer, An iterative procedure for the polygonal approximation of plane curves, *Computer graphics and image processing*, vol. 1, no. 3, pp. 244–256, 1972.
- [22] J. Yu, G. Chen, X. Zhang, W. Chen, Y. Pu, An improved Douglas-Peucker algorithm aimed at simplifying natural shoreline into direction-line, *21st International Conference on Geoinformatics*. (2013), 1-5.
- [23] Y. Zhao, C. Xie, Y. Qiao, Douglas-Peucker algorithm based on extreme points, *Software Guide*. (2008), 60-62.